



# Multi-dimensional Inversion Modeling of Surface Nuclear Magnetic Resonance (SNMR) Data for Groundwater Exploration

Warsa, Hendra Grandis, Wahyudi W. Parnadi & Djoko Santoso

Applied Geophysics Research Group, Faculty of Mining and Petroleum Engineering,  
Institut Teknologi Bandung, Jalan Ganesa No.10, Bandung 40132, Indonesia  
Email: warsa@gf.itb.ac.id

**Abstract.** Groundwater is an important economic source of water supply for drinking water and irrigation water for agriculture. Surface nuclear magnetic resonance (SNMR) sounding is a relatively new geophysical method that can be used to determine the presence of culturally and economically important substances, such as subsurface water or hydrocarbon distribution. SNMR sounding allows the determination of water content and pore size distribution directly from the surface. The SNMR method is performed by stimulating an alternating current pulse through an antenna at the surface in order to confirm the existence of water in the subsurface. This paper reports the development of a 3-D forward modeling code for SNMR amplitudes and decay times, after which an improved 2-D and 3-D inversion algorithm is investigated, consisting of schemes for regularizing model parameterization. After briefly reviewing inversion schemes generally used in geophysics, the special properties of SNMR or magnetic resonance sounding (MRS) inversion are evaluated. We present an extension of MRS to magnetic resonance tomography (MRT), i.e. an extension for 2-D and 3-D investigation, and the appropriate inversions.

**Keywords:** *decay time; hydrogeological parameters; MRS; SNMR; water content.*

## 1 Introduction

Groundwater is an important natural resource all around the world. Quantification and qualification of groundwater and hydro-geological parameters of aquifers are necessary to manage and preserve groundwater resources. Furthermore, information about the availability of groundwater resources and how they can be exploited is essential for a sustained socio-economic development of any area, whether urban or rural. For this purpose, geophysical methods provide a wide range of very useful and powerful tools that, when used correctly and in the right situation, will produce useful information.

Along with the widening of the application range of geophysical methods, particularly with respect to the investigation of derelict and contaminated land,

---

Received February 26<sup>th</sup>, 2013, 1<sup>st</sup> Revision July 25<sup>th</sup>, 2013, 2<sup>nd</sup> Revision December 6<sup>th</sup>, 2013, Accepted for publication February 11<sup>th</sup>, 2014.

Copyright © 2014 Published by ITB Journal Publisher, ISSN: 2337-5779, DOI: 10.5614/j.eng.technol.sci.2014.46.2.1

the sub-discipline of environmental geophysics has developed [1]. These measurements can be used to infer the porosity, permeability, chemical constitution, stratigraphy, geologic structure, and various other properties of volume materials near the earth's surface. In groundwater exploration they can be employed to predict groundwater levels, physical parameters of aquifers, seawater intrusion, contaminants from the land surface, and land subsidence caused by human activities (mainly through the removal of subsurface water).

A new geophysical method that can be applied for this purpose is SNMR. The SNMR method is conducted on a test site to yield the geometry, water content and hydraulic permeability of an aquifer [2,3]. Besides allowing a more detailed and reliable assessment of aquifers, the SNMR method may also be used to detect changes of water content and hydrogeological parameters.

To improve the capabilities of the SNMR method, we have carried out a research to study the response of 2-D and 3-D models, i.e. the SNMR relaxation signal for various locations of the antenna loop. The main aim of this research was to improve the ability of the SNMR method to determine groundwater parameters in the subsurface. The emphasis of the research was on the development of a groundwater modeling program that allows to determine the initial amplitude and decay time of an SNMR signal for the 3-D water distribution in dependence of the pulse moment. Finally, we have developed a 2-D and 3-D inversion to increase the interpretation of the SNMR method.

## 2 Methodology

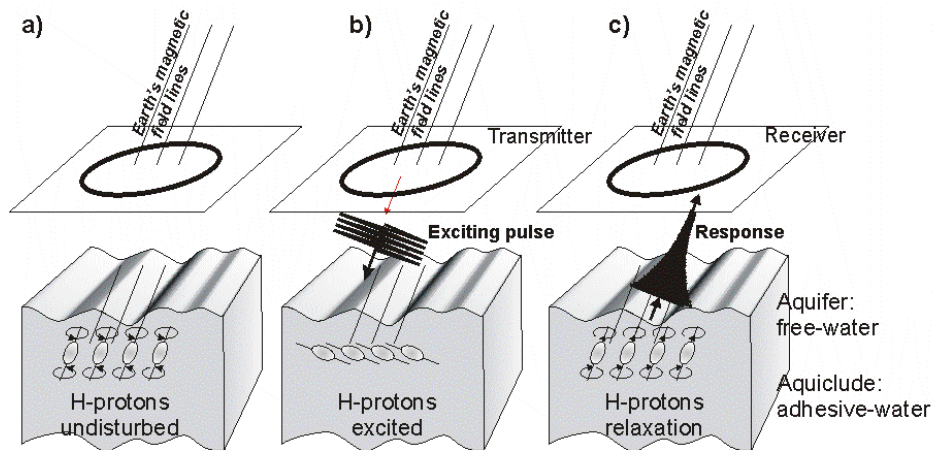
Surface nuclear magnetic resonance (SNMR) sounding is a geophysical method that is aimed at determining hydro-geological parameters from magnetic resonance measurements. This method is based on the principle of proton magnetic resonance in the Earth's field of hydrogen  $1H$  atoms contained in groundwater  $H_2O$  molecules. An NMR signal, stimulated by an alternating current pulse through an antenna at the surface, confirms the existence of water in the sub-surface. The amplitudes of the NMR signal are directly related to the water content, while the decay times are linked to pore size, grain size and, therefore, to hydraulic conductivities. The phases are related to the electrical conductivity; this measurement can be used qualitatively and quantitatively [4] (Table 1).

Figure 1 shows the three stages of SNMR measurement. The equilibrium of hydrogen protons (Figure 1(a)) is excited by an alternating current pulse through the antenna at the surface to confirm the existence of water in the sub-surface, as shown in Figure 1(b). After termination of the exciting pulse, the

response field due to the relaxation of the precessing hydrogen is measured (Figure 1(c)).

**Table 1** Physical parameters determined with SNMR

Measured quantity (vs. pulse moment)	Physical parameter (vs. depth)
Amplitude of the SNMR signal $E_0(q)$	Water content
Decay time constant of signal $T_2^*$	Mean pore size
Phase shift between signal and current $\varphi$	Rock layer resistivity



**Figure 1** Schematic of the SNMR field measurement principle using a coincident transmitter and receiver circular loop in three stages. a) H-protons undisturbed in equilibrium, b) H-protons excited by AC pulse through antenna, and c) after termination the response field due to relaxation is measured [5].

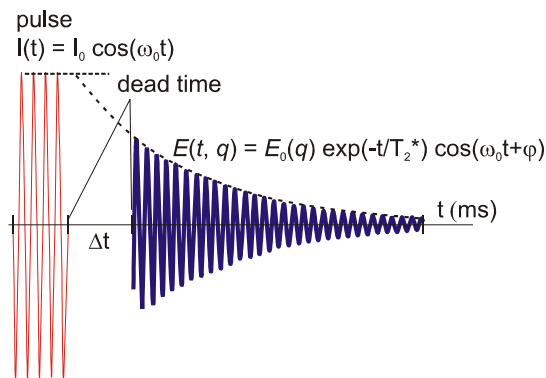


**Figure 2** Time diagram of SNMR signal measurements.

In Figure 2, a time diagram of the current impulse and received signal is shown. The initial amplitude  $E_0$  of the signal corresponds to the water content in the sub-surface [6,7]. The decay time  $T_2^*$  (spin-spin relaxation time) of the SNMR signal corresponds to pore size. The fundamental integral-equation that governs the amplitudes  $E_0(q)$  of the nuclear magnetic resonance as a function of the pulse moment  $q$  is given by [8]:

$$E(t, q) = E_0(q)e^{-t/T_2^*(q)} = \omega_0 M_0 \int_V e^{-t/T_2^*(\mathbf{r})} f(\mathbf{r}) \cdot B_{\perp}(\mathbf{r}) \cdot \sin \theta(\mathbf{r}) dV, \quad (1)$$

in which  $\omega_0$  is the local Larmor frequency of the hydrogen protons and  $M_0$  is the nuclear magnetization of the protons. The water content and the decay time for a unit volume at point  $\mathbf{r}$  in the subsurface are given by  $f(\mathbf{r})$  and  $T_2^*(\mathbf{r})$  respectively.  $B_{\perp}(\mathbf{r})$  states the component of the incident exciting magnetic field perpendicular to the Earth's geomagnetic field. The tilt angle of the protons is given by  $\theta(\mathbf{r}) = 0.5\gamma B_{\perp}(\mathbf{r}) q$ . Increasing the pulse moment  $q$  ( $q = I_0 \tau$ , where  $I_0$  and  $\tau$  are the amplitude and duration time of the current pulse respectively) increases the depth of penetration of the method.

### 3 3-D Forward Modeling

Interpreting SNMR data consists of determining the water content of each layer, in the hypothesis where the underground is stratified at the scale of the loop dimensions. The inversion consists of processing the raw data for the whole set of pulse moments corresponding to the various depths of investigation. However, some parameters are well defined, such as the product of the thickness of a thin layer and its water content. The development of a 3-D forward modeling of SNMR initial amplitudes and decay times was based on the work of Eikam [9], which can be used for two and three-dimensional interpretation of SNMR surveys. The formulation is reduced to a finite dimensional matrix problem by considering a finite number of cells with constant spin density (water content and decay time). The 3D forward modeling is then calculated by generating synthetic data for several spin density distributions. This allows to analyze the spatial signal sensitivity of the method and shows the limits and problems of the 1-D inversion and the interpretation of the 2-D and 3-D structures.

We have introduced a 3-D forward modeling of the initial SNMR amplitudes and decay times [9-11]. A prismatic three-dimensional body model is divided into small cubic cells of dimension  $\Delta V = \Delta x \Delta y \Delta z$ . The water content  $f(x, y, z)$  and the decay times  $T_2^*(x, y, z)$  are assumed to be constant in each cell. Then the integral equation is approximated by the finite summation

$$E(t, q) = \omega_0 M_0 \sum_z \sum_y \sum_x e^{-t/T_2^*(x, y, z)} f(x, y, z) \cdot B_{\perp}(x, y, z) \sin \theta(x, y, z) \Delta x \Delta y \Delta z. \quad (2)$$

From this relation, the complete SNMR signal can be calculated as a function of a three-dimensional distribution of the water content  $f(x, y, z)$  and decay time  $T_2^*(x, y, z)$  in the subsurface. The initial amplitude for  $t = t_0$ , the start of the record, is then given by:

$$E_0(q) = \omega_0 M_0 \sum_z \sum_y \sum_x f(x, y, z) \cdot B_{\perp}(x, y, z) \sin \theta(x, y, z) \Delta x \Delta y \Delta z. \quad (3)$$

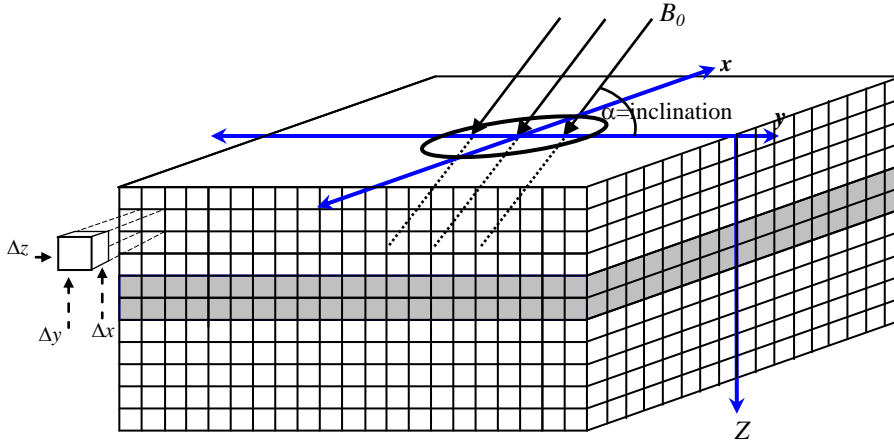
The inner part of the integral is commonly written as the product of a kernel function and the water content

$$E_0(q) = \sum_z \sum_y \sum_x f(x, y, z) \cdot K_{3D}(q; x, y, z) \Delta x \Delta y \Delta z, \quad (4)$$

where  $K_{3D}(q; x, y, z) = \omega_0 M_0 \sum_z \sum_y \sum_x B_{\perp}(x, y, z) \sin \theta(x, y, z) \Delta x \Delta y \Delta z$ .  $\Delta x$ ,  $\Delta y$  and  $\Delta z$  describe the side-length of volume element  $\Delta V$ .

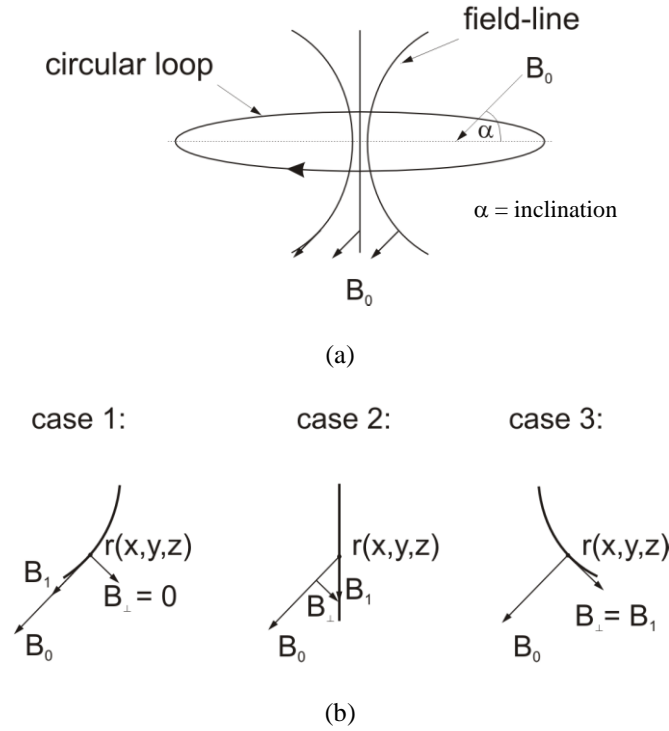
### 3.1 Perpendicular Component of Magnetic Field

Figure 3 represents the 3-D model discretization for which the SNMR model has been calculated using a one-turn circular loop in a geomagnetic field of 48000 nT at an inclination of  $60^\circ$  and a declination of  $0^\circ$  in a low conductive



**Figure 3** Distribution of subsurface in small cube with volume  $\Delta V_n$  for calculating initial amplitude  $E_0$  and decay times  $T_2^*$  of aquifer.

half-space. The AC magnetic field  $B_I(r, t)$  generated by the transmitter coil causes the nuclear magnetization of proton  $M_N$  to tip away from  $B_0$  at the (angular) Larmor frequency  $\omega_L = 2\pi f_L = \gamma B_0$ . The incident magnetic field at the Larmor frequency can be absorbed by the nucleus. Upon absorption of a unit of magnetic field, the vector of magnetic moment is deflected from its equilibrium position in static magnetic field  $B_0$ , reflecting the changed energy state of the nucleus.



**Figure 4** (a) Magnetic field for a circular current; (b) Possible cases for perpendicular component of circular loop.

The magnetic field of circular loops consists of parallel and orthogonal (perpendicular) components aligned with the geomagnetic field as shown in Figure 4(a). Figure 4(b) shows the possible cases of the values of the perpendicular components of the magnetic field. In general, a magnetic field orthogonal to a geomagnetic field can be described by:

$$B_{\perp}(r) = B_1(r) - B_0(r) \cdot B_1(r) . \tag{5}$$

$B_{\perp}(r)$  is the component of the incident exciting field  $B_I(r)$  perpendicular to the static magnetic field  $B_0$  of the Earth. In a conductive medium,  $B_{\perp}(r)$  is

composed of the primary field of the loop and the induced field in case of high conductivity, which causes the phase shift  $\varphi(r)$  with respect to the excitation field. Furthermore, the tilt angle of the deflected hydrogen spins for a unit volume at the point  $r$  is given by

$$\theta(q, r) = 0.5\gamma_p B_{\perp}(r)q. \quad (6)$$

Pulse moment  $q$  [A.s] determines the depth of investigation. A higher pulse moment derives the SNMR response from a greater depth. With the existing equipment, pulse moment  $q$  can range from 60 to 20,000 A.ms depending on the loop size and the electrical conductivity of the subsurface.

### 3.2 Distribution of Proton Magnetic Resonance

In the following forward computations, we took a magnitude of the Earth's magnetic field,  $B_0$ , 48000 nT to be tilted by  $30^\circ$  northward away from the vertical (declination  $0^\circ$ , inclination  $60^\circ$ ), with Larmor frequency  $f_L = 2042.83$  Hz. The transmitter and receiver loops are circular coincident with a diameter of 100 m. The solid earth model is a homogeneous non-conducting half-space. Genuinely realistic simulations, however, would require the conductivity to be a variable function of depth, particularly because it is a strong function of water content.

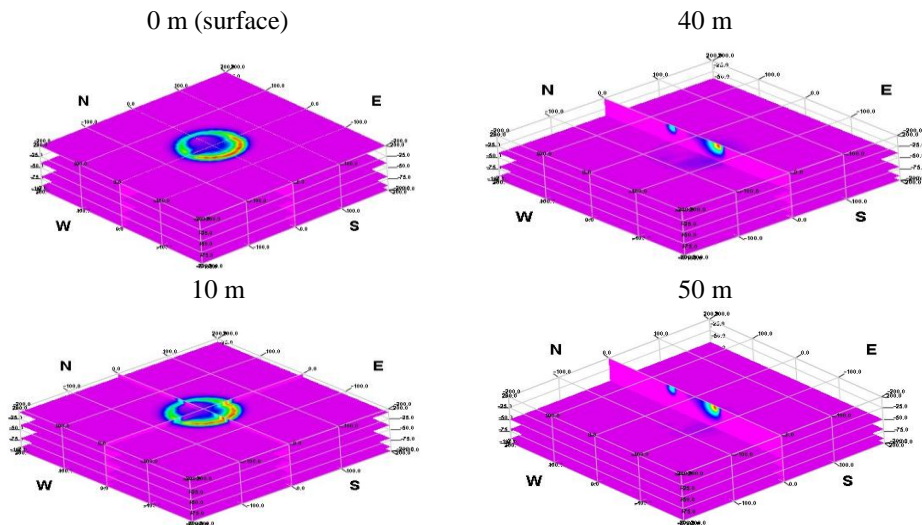


**Figure 5** Sensitivity of 3-D SNMR sounding at various depths of the forward modeling using a coincident circular loop (diameter = 100 m) at pulse moment  $q = 1$  A.s for the homogeneous half-space model.

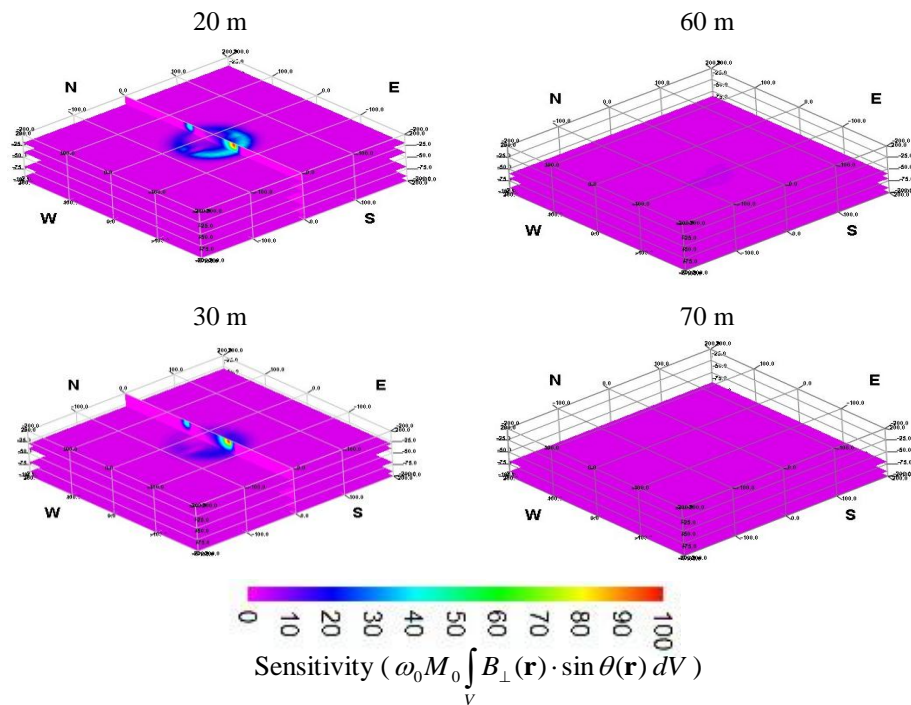


**Figure 5 Continued.** Sensitivity of 3-D SNMR sounding at various depths of the forward modeling using a coincident circular loop (diameter = 100 m) at pulse moment  $q = 1$  A.s for the homogeneous half-space model.

The representations of excited proton distribution or kernel are shown in Figure 5. Figure 5 shows 3-D sensitivity of the forward modeling at various depths using a coincident circular loop (diameter = 100 m) at pulse moment  $q = 1$  A.s for the homogeneous half-space model.

#### 4 Water Layer Model

In order to check the numerical accuracy of the forward code, the synthetic data were compared with data generated by the 1-D code of Mohnke [12] (Figure 6). Coil diameter 100 m, current 1 A, geomagnetic field  $B_0 = 48000$  nT, and  $\Delta x = \Delta y = \Delta z = 1$  m.

Using the formula in Eq. (2) it is possible to compute the initial response amplitude  $E_0(q)$  and decay time  $T_2^*(q)$  of a water layer at various depths and thicknesses. The effects of a water layer with finite thickness and depth variations are shown in Figure 7 and 8. One-layer models have been used to represent an aquifer having a water content (WC) of 40 vol.% and decay time of



100 ms. The surrounding material has a water content of 5 vol.% and decay times of 30 ms.

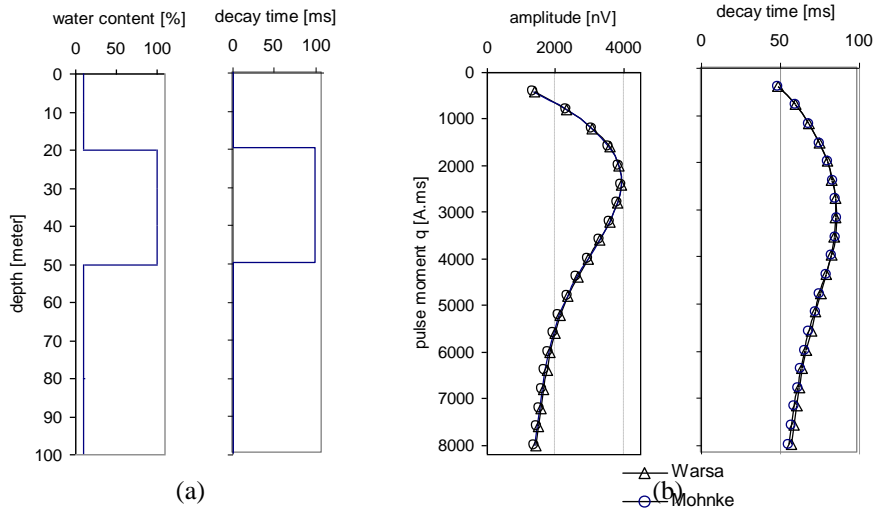


**Figure 6** Comparison with the forward code of Mohnke: (a) 1-D model of horizontal layer, (b) synthetic SNMR amplitudes (left) and decay times (right);  $B_0 = 48000$  nT;  $I = 60^\circ$ ; circular loop, diameter 100 m.

#### 4.1 1-D Water Layer with Thickness Variation

The depth ( $h$ ) of a 1-D water layer model has been fixed at 10 m for various layer thicknesses ( $\Delta h_i$ ). The thickness of the water layer increases from 10 m ( $\Delta h_1$ ) to 50 m ( $\Delta h_5$ ) in steps of 10 m. Figure 7 shows that the maximum position

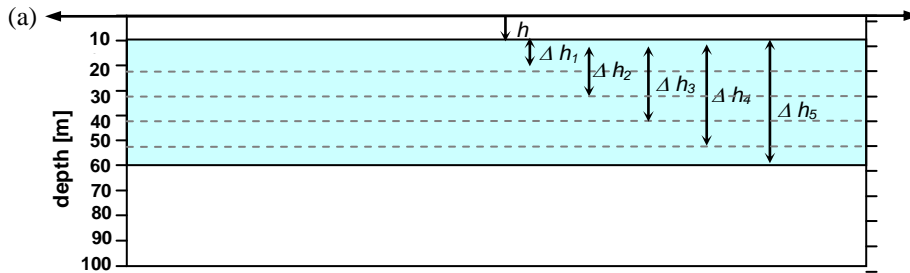


**Figure 7** (a) 1-D water layer at a depth of 10 m for various layer thicknesses with 40 vol.% of water content and 100 ms of decay time, (b) NMR response for amplitude (left) and decay time (right) as a function of pulse moment for all 1-D water layers with depth variation.

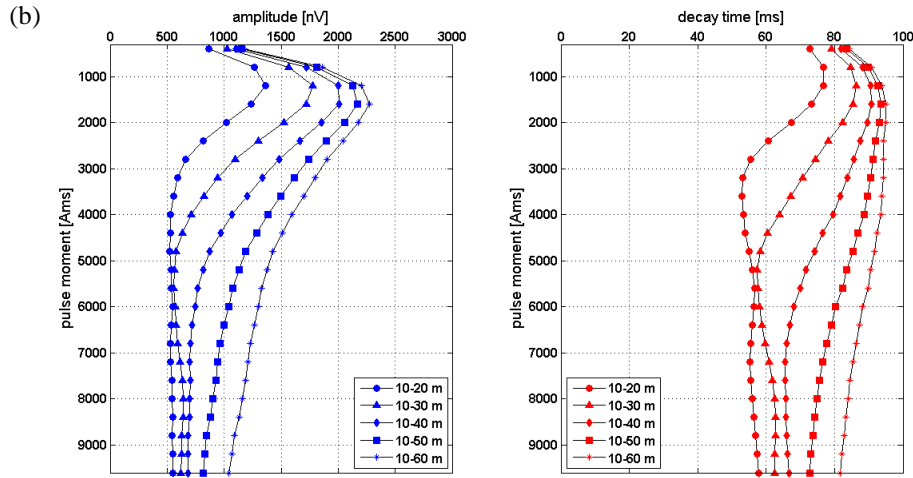


**Figure 7 Continued.** (a) 1-D water layer at a depth of 10 m for various layer thicknesses with 40 vol.% of water content and 100 ms of decay time, (b) NMR response for amplitude (left) and decay time (right) as a function of pulse moment for all 1-D water layers with depth variation.

of the response, amplitude and decay time vs. pulse moment, is shifted to a higher value of pulse moment. At a water layer depth of 10-20 m ( $h = 10$  m), the maximum amplitude value is 1300 nV at pulse moment 1400 A ms. The maximum value of amplitude and decay time, of course, increases as the thickness of the layer increases.

Figure 8 represent the NMR response of a water layer with a constant thickness ( $\Delta h = 10$  m). The depth is shifted from 10 m ( $h_1$ ) to 50 m ( $h_5$ ) by steps of 10 m. When the depth increases, the response of both amplitude and decay time has a wider curve and the peak value is lower. The peak is also shifted to a higher value of pulse moment as the depth of the water layer increases.

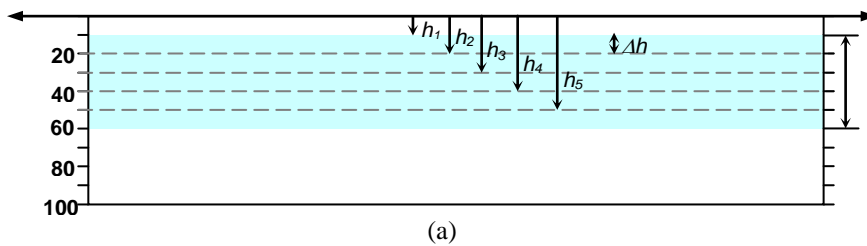


**Figure 8** (a) 1-D water layer for various layer depths with a constant thickness having 40 vol.% of water content and 100 ms of decay time, (b) NMR response of initial amplitude (left) and decay time (right) as a function of pulse moment.

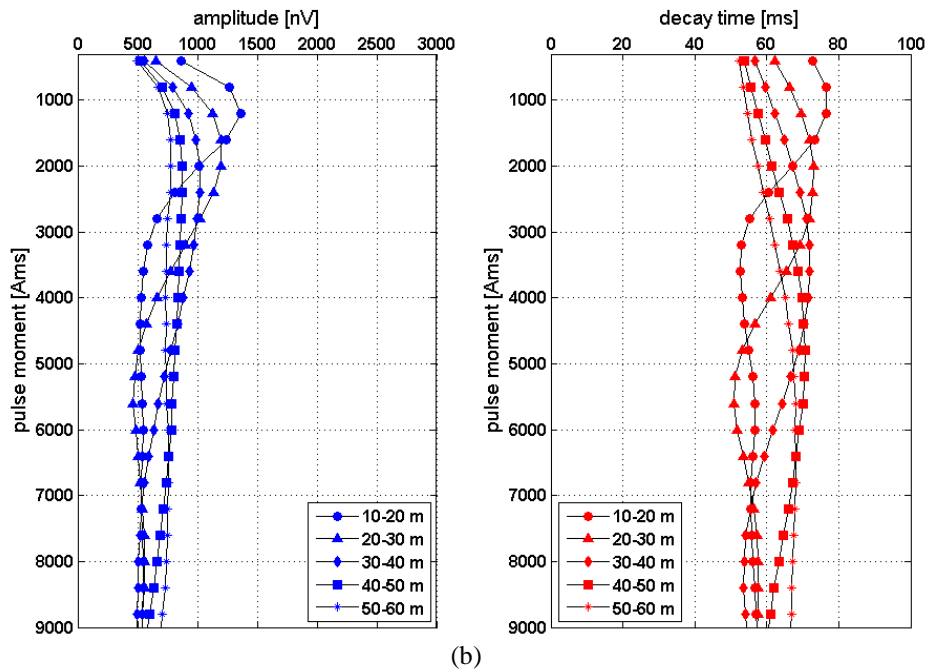


**Figure 8** *Continued.* (a) 1-D water layer for various layer depths with a constant thickness having 40 vol.% of water content and 100 ms of decay time, (b) NMR response of initial amplitude (left) and decay time (right) as a function of pulse moment.

## 5 2-D and 3-D Inversion

The first task of this research was to extend the initial amplitude 3-D forward modeling code to decay times ( $T_2^*$ ) for SNMR. This scheme can be used for a 2- and 3-dimensional interpretation of SNMR surveys. For a better understanding of the capabilities of the method, we calculated the SNMR response of 2-D and 3-D models, i.e. the SNMR relaxation signals for various locations of the antenna loop. The 3-D forward modelling was then calculated by generating synthetic data for several spin density distributions. This allowed us to analyse the spatial signal sensitivity of the method and show the limits and problems of the 1-D inversion and the interpretation of the 2-D and 3-D structures [9].

In geophysics, the conditions are mostly mixed; i.e. some model parameters are over-determined and some are under-determined. Here a set of estimated solutions:

$$\mathbf{m}^{est} = \mathbf{G}^T (\mathbf{G}^T \mathbf{G})^{-1} \mathbf{d}^{obs} \quad (7)$$

can predict the observed data perfectly, where  $\mathbf{d}$  is the modeled data,  $[d_i]$ ,  $i = 1, 2, \dots, N$ ;  $\mathbf{m}$  is the model parameter,  $[m_j]$ ,  $j = 1, 2, \dots, M$ ; and  $\mathbf{G}$  is the relation of the data to the model parameter (physical model),  $[G_{ij}]$ . For the inversion of the SNMR data, the Tikhonov regularization method was used in order to minimize the number of measurements [7,13] without loss of accuracy. Here, the function to be minimized consisted of two terms, taking both data fit and model smoothness into account:

$$\|\mathbf{G}\mathbf{m}^{est} - \mathbf{d}^{obs}\|_2^2 + \alpha^2 \|\mathbf{L}\mathbf{m}\|_2^2 \quad (8)$$

The order of the Tikhonov solution and, therefore, also the degree of smoothness, is defined by matrix  $\mathbf{L}$  that acts as a derivate operator. For  $\mathbf{L} = \mathbf{I}$  ( $\mathbf{I}$ : unit matrix), the model roughness is taken into account and referred to as the Tikhonov solution of zero<sup>th</sup> order. For the MRS standard approach, in most simple cases,  $\mathbf{d}$  and  $\mathbf{m}$  may contain  $\mathbf{d}$  = initial amplitude (for different excitation intensities);  $\mathbf{m}$  = water content (of horizontal layers with fixed boundaries). A modified Levenberg-Marquardt algorithm used to find the parameters that minimize the objective function is as follows:

$$\mathbf{m} = (\mathbf{G}^T \mathbf{G} + \alpha \mathbf{I})^{-1} \mathbf{G}^T \mathbf{d}, \quad (9)$$

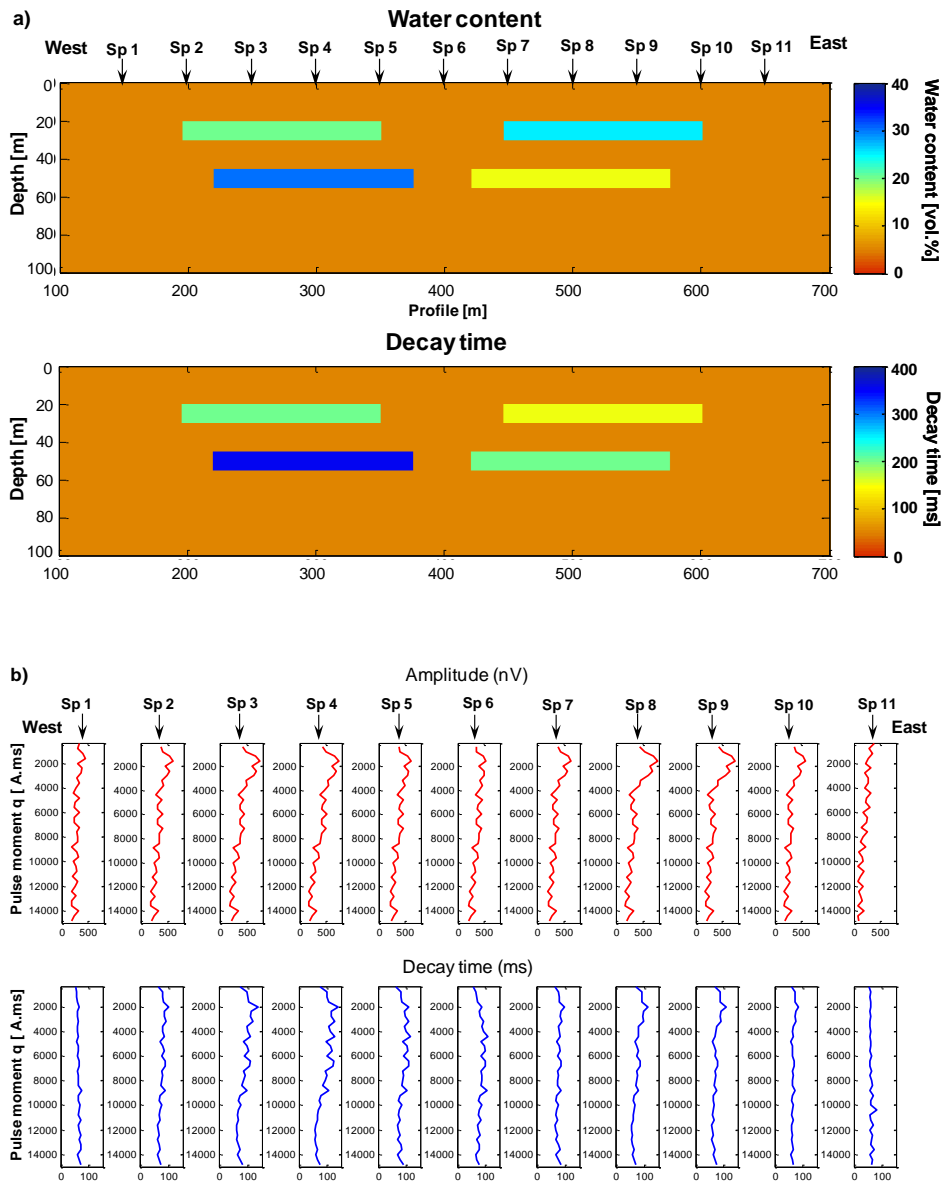
where  $\alpha$  is the damping parameter and  $\mathbf{I}$  is the identity matrix.

We performed an inversion of the 2-D and 3-D synthetic signals computed for a multi water lens model. SNMR measurements were carried out at the surface. The synthetic SNMR data have been calculated using a circular loop (one turn, diameter  $d = 50$  m) in a geomagnetic field of 48000 nT, at an inclination of  $60^\circ$  and declination of  $0^\circ$  in a low conductive half-space.

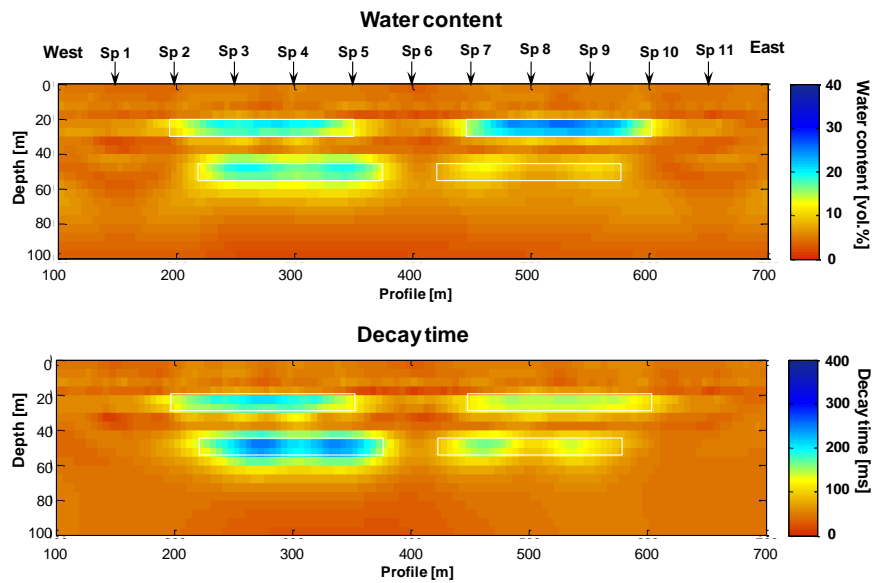
## 5.1 2-D Inversion Modeling

Figure 9(a) shows a *multi water lens* synthetic model with variable depth, water content and decay time. The synthetic data of initial amplitude and decay time versus pulse moment  $q$  are shown in Figure 9(b).

The 2-D inversion results of water content and decay time are shown in Figure 10 (top) and (bottom) respectively. The results place the multi-water lens-feature at the correct location as well as the physical properties of water content and decay time.



**Figure 9** (a) Synthetic multi water lens model for various depths, water contents and decay times, (b) Synthetic SNMR data of amplitude (top) and decay time (bottom) generated by forward modeling.



**Figure 10** 2-D inversion model of water content (top) and decay time (bottom).

## 5.2 3-D Inversion Modeling

Following the 2-D inversion, a full 3-D inversion was applied. The regularized inversion scheme uses the 3-D integral equation method for modeling the nuclear magnetic resonance fields and their sensitivities. The 3-D synthetic model of water content and decay time is shown in Figure 11. The 3-D inversion domain covered the profile from 0 m to 1000 m, was 1000 m wide and extended from the surface down to 100 m depth. The inversion domain was discretized into cells of 10 m x 10 m x 10 m size in the  $x$ ,  $y$  and  $z$  directions, respectively.

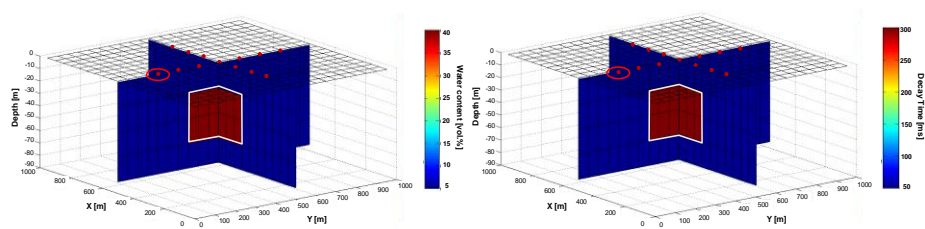


**Figure 11** 3-D synthetic model of water content (left) and decay time (right).

3-D inversion model of water content and decay time are shown in Figure 12. Figure 13 shows slices of 3-D inversion model of water content and decay time at a depth 20 m, 30 m and 40 m. The SNMR 3-D inversion result is in general agreement with that obtained by 2-D inversion, particularly the water content and decay time features between 20 m and 60 m. The lateral placement correlates well with the known location of the 3-D water lens model. The 3-D inversion result places the water-lens feature at the correct depth.

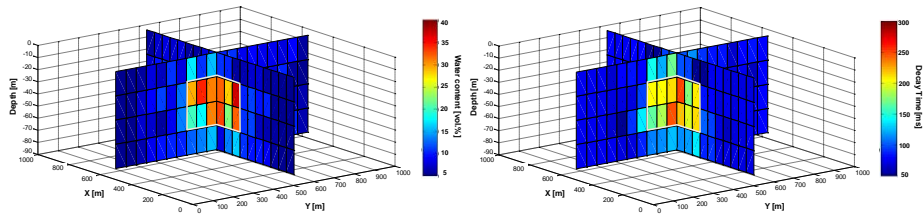


**Figure 12** 3-D inversion model of water content (left) and decay time (right).

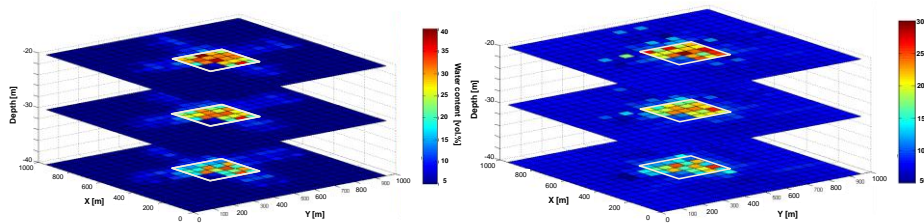


**Figure 13** Slices at a depth 20 m, 30 m and 40 m of 3-D inversion model of water content (left) and decay time (right).

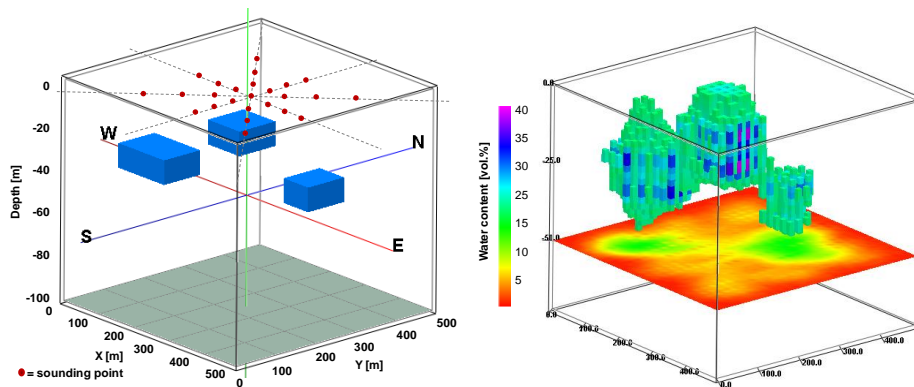


**Figure 14** 3-D synthetic model (left) and 3-D inversion model (right) of water content.

A 3-D multi water lens model with a water content of 40%, as shown in Figure 14 (left), was considered. The 3-D inversion modeling result of the water content is shown in Figure 14 (right). Figure 15 shows a plan view at a depth of 10, 20, 30, 40, 50 and 60 m. The lateral placement correlates well with the known location of the 3-D water lens model. The 3-D inversion result places the water lens feature at the correct depth. With the inclusion of more detailed structural information about water content and decay time, we believe the high quality of the data will enable elucidation of the subsurface in more detail.

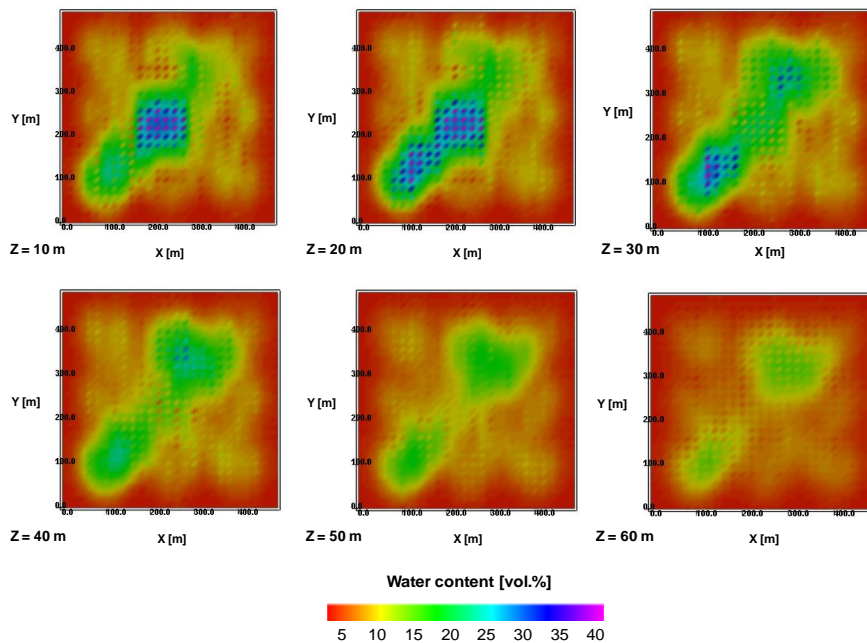


**Figure 15** Plan view of 3-D water content model at  $z = 10, 20, 30, 40, 50$  and  $60$  m derived approximate 3-D inversion for the model shown in Figure 14.

## 6 Conclusions

We have described the key elements of a multi-dimensional SNMR inversion scheme as an improvement of the 2-D tomographic method [14]. By using simulated data derived from a measurement series, a rapid new scheme accurately reconstructed the boundaries and average value of water content and decay time.

Multi-dimensional modeling of SNMR data is necessary to predict the SNMR signal response of aquifers. For optimization of field layouts, a forward modeling method is used for appropriate measurement of a given 2-D and 3-D situation. Similar to most geophysical surface methods, 3-D SNMR has a



limited resolution, but it is effective for investigating water-saturated geological formations larger than several tens of meters [15]. For demonstration purposes, we have presented an improved 2-D and 3-D inversion algorithm using the Levenberg-Marquardt algorithm. The inversion results place the water content feature at the correct depth and volume.

In the near future, this inversion scheme will be applied to SNMR field data. Subsequently, the SNMR method can be applied to detect subsurface water in suitable geological formations to depths of up to 100 m and more, depending on the presence of natural and cultural electromagnetic noise.

### **Acknowledgements**

This work was supported in part by a Chevron Scholarship and was a continuation of earlier works performed at the Applied Geophysics Department of the Technical University Berlin, Germany. The authors would like to thank their advisor Prof. Dr. Ugur Yaramanci for providing a research environment for the SNMR project that is both challenging and exceptionally rewarding.

The authors would also like to thank the journal reviewers for their constructive comments on an earlier version of this paper.

### **Nomenclature**

NMR : Nuclear Magnetic Resonance

SNMR : Surface Nuclear Magnetic Resonance

MRS : Magnetic Resonance Sounding

MRT : Magnetic Resonance Tomography

### **References**

- [1] Steeples, D.W., *Engineering and Environmental Geophysics at The Millennium*, Geophysics, **66**(1), pp. 31-35, 2001.
- [2] Yaramanci, U., Lange, G. & Hertrich, M., *Aquifer Characterisation Using Surface NMR Jointly with other Geophysical Techniques at the Nauen/Berlin Test Site*, Journal of Applied Geophysics, **50**, pp. 47-65, 2002.
- [3] Yaramanci, U., Lange, G. & Knödel, K., *Surface NMR within a Geophysical Study of an Aquifer at Haldensleben (Germany)*, Geophysical Prospecting, **47**, pp. 923-943, 1999.
- [4] Braun, M. & Yaramanci, U., *Inversion of Resistivity in Magnetic Resonance Sounding*, Journal of Applied Geophysics, **66**, pp. 151-164, 2008.

- [5] Lange, G., Yaramanci, U. & Meyer, R., *Surface Nuclear Magnetic Resonance*. In: Knödel, K., Lange, G. & Voigt, H.J. (Eds): *Environmental Geology-Handbook of Field Methods and Case Studies, 4 Geophysics*, Springer, pp. 403-430, 2007.
- [6] Schirov, M. & Legchenko, A., *A New Non-invasive Groundwater Detection Technology for Australia*, *Exploration Geophysics*, **22**, pp. 333-338, 1991.
- [7] Legchenko, A.V. & Shushakov, O.A., *Inversion of Surface NMR Data*, *Geophysics*, **63**, pp. 75-84, 1998.
- [8] Weichmann, P.B., Lively, E.M. & Ritzwoller, M.H., *Theory of Surface Nuclear Magnetic Resonance with Application To Geophysical Imaging Problem*, *Physical Review E*, **62**(1), pp. 1290-1312, 2000.
- [9] Eikam, A., *Modellierung von SNMR-Anfangsamplituden*, Master's Thesis, Technical University Berlin, 1999.
- [10] Warsa, W., Mohnke, O. & Yaramanci, U., *3-D Modelling of Surface NMR Amplitudes and Decay Times*, *International Water Resources and Environmental Research ICWRER 2002*, **III**, Eigenverlag des Forums für Abfallwirtschaft und Atlanten e.V., Dresden, pp. 209-212, 2002.
- [11] Warsa, W., & Grandis, H., *Sensitivity Study of 3-D modeling for Multi-D Inversion of Surface NMR*, *Proceedings of International Conference on Physics and Its Applications (ICPAP) 2011*, *AIP Conference Proceeding*, **1454**, New York, pp. 130-133, 2011.
- [12] Mohnke, O., *Entwicklung und Anwendung eines neuen Inversionsverfahrens für Oberflächen-NMR Sondierungen*, Master's Thesis, Technical University Berlin, 1999.
- [13] Yaramanci, U. & Petke, M., *Improvements in Inversion of Magnetic Resonance Exploration-Water Content, Decay Time, and Resistivity*, *Journal of Earth Science*, **20**(3), pp. 592-605, 2009.
- [14] Hertrich, M., Braun, M., Günther, T., Green, A.G. & Yaramanci, U., *Surface Nuclear Magnetic Resonance Tomography*, *IEEE Transactions on Geoscience and Remote Sensing*, **45**(11), pp. 3752-3759, 2007.
- [15] Legchenko, A., Descloitres, M., Vincent, C., Guyard, H., Garambois, S., Chalikakis, K., & Ezersky, M., *Three-Dimensional Magnetic Resonance Imaging for Groundwater*, *New Journal of Physics*, IOP Publishing Ltd and Deutsche Physikalische Gesellschaft, **13**, pp.1-18, 2011.